Room-temperature operation of $\lambda \approx 7.5\ \mu$m surface-plasmon quantum cascade lasers

M. Bahriz, V. Moreau, J. Palomo, and R. Colombelli[a)]
Institut d'Electronique Fondamentale, UMR8622 CNRS, Université Paris Sud, 91405 Orsay, France

D. A. Austin, J. W. Cockburn, and L. R. Wilson[b)]
Department of Physics and Astronomy, University of Sheffield, Sheffield S3 7RH, United Kingdom

A. B. Krysa and J. S. Roberts
EPSRC National Centre for III-V Technologies, Department of Electronic and Electrical Engineering, University of Sheffield, Sheffield, S1 3JD, United Kingdom

(Received 1 February 2006; accepted 24 March 2006; published online 2 May 2006)

We report the pulsed, room-temperature operation of $\lambda \approx 7.5\ \mu$m quantum cascade lasers (QCLs) in which the optical mode is a surface-plasmon polariton excitation. Previously reported devices based on this concept operate at cryogenic temperatures only. The use of a silver-based electrical contact with reduced optical losses at the QCL emission wavelength allows a reduction of the laser threshold current by a factor of 2 relative to samples with a gold-based contact layer. As a consequence, the devices exhibit room-temperature operation with threshold current densities $\sim 6.3\ \mathrm{kA/cm^2}$. These devices could be used as all-electrical surface-plasmon generators at midinfrared wavelengths. © *2006 American Institute of Physics*. [DOI: 10.1063/1.2198016]

Surface-plasmon polaritons are mixed electromagnetic modes that originate from the coupling between the electromagnetic field and plasmonic excitations, typically in metallic thin films. Their nature is intrinsically nonradiative, and their electric field distribution is that of an exponential decay away from the interface between the metal and the dielectric material.[1] Such behavior is dictated by Maxwell equations for the case of an interface between two materials with dielectric constants of opposite signs, such as a metal-semiconductor interface.

The recent intensive study of surface-plasmon related effects[2] is essentially motivated by two characteristics: (i) their ability to confine light down to subwavelength dimensions[3] and (ii) the surface-field enhancement.[4] The second property is currently exploited in surface-enhanced Raman spectroscopy and surface-plasmon-enhanced fluorescence spectroscopy. In addition, surface-plasmon-enhanced light emitting diodes have been recently demonstrated at $\lambda \approx 470$ nm.[5]

To date, surface-plasmon excitations have been generated by optical means. However, their intrinsic *nonradiative* nature complicates the task since surface plasmons do not couple directly with incoming or outcoming electromagnetic waves. The use of gratings,[1] is therefore necessary. A room-temperature, all-electrical generator of surface plasmons would be therefore an advance in the field. The obvious way to obtain emission and, even better, stimulated emission of surface plasmons is to couple the surface-bound electromagnetic mode with a material that exhibits optical gain.[6]

Interestingly, surface plasmons are already used at very long wavelengths ($\lambda \approx 70-200\ \mu$m) as a guiding solution for terahertz quantum cascade (QC) lasers. In this case surface plasmons are coupled to a material that exhibits optical gain (the laser active region), thanks to the intrinsic transverse-magnetic character of the light emitted through intersubband transitions in semiconductor quantum wells. Figure 1 clarifies how the surface-plasmon dispersion relation allows operation of the devices at these very long wavelengths. The bulk plasmon frequency of the metal is momentum independent, and it lies in the 3–5 eV energy range (UV range of the electromagnetic spectrum). On the other hand, surface plasmons exhibit, at low k, an acousticlike behavior asymptotic to the light line in the semiconductor. Such a behavior allows the waveguide mode of the laser to match the surface-plasmon momentum at midinfrared and terahertz frequencies.

The surface-plasmon damping along the propagation direction can be approximated with the following formula:[7]

$$\alpha \approx \frac{4\pi}{\lambda}\frac{n_m n_d^3}{k_m^3}, \tag{1}$$

where k_m and n_m are the imaginary and real parts of the metal index of refraction, n_d is the real part of the semiconductor index of refraction, and λ is the wavelength. The $1/k^3\lambda$ dependence of the propagation losses makes this an extremely low-loss waveguiding solution in the terahertz range of the electromagnetic spectrum. However, these devices do not work at room temperature, and their operating frequency is too low for existing plasmonic applications.[2–4] Surface plasmons have also been used for waveguiding at shorter wavelengths ($\lambda \approx 8-11\ \mu$m),[7] but pulsed, room-temperature operation has not been achieved yet. In this letter we show that by carefully choosing the metal surface-plasmon guiding layer (silver was used in this case), and by combining it with a high performance semiconductor material, it is possible to obtain pulsed, room-temperature operation of surface-plasmon QC lasers at shorter wavelengths ($\lambda \approx 7.5\ \mu$m).

The laser structure (MR2230) described here was grown by low pressure (150 torr) metal organic vapor phase epitaxy (MOVPE) using an $In_{0.53}Ga_{0.47}As/Al_{0.48}In_{0.52}As$ lattice matched to a highly doped InP substrate. A 2-μm-thick low-

a)Electronic mails: colombel@ief.u-psud.fr and colombel@mailaps.org
b)Electronic mail: luke.wilson@sheffield.ac.uk

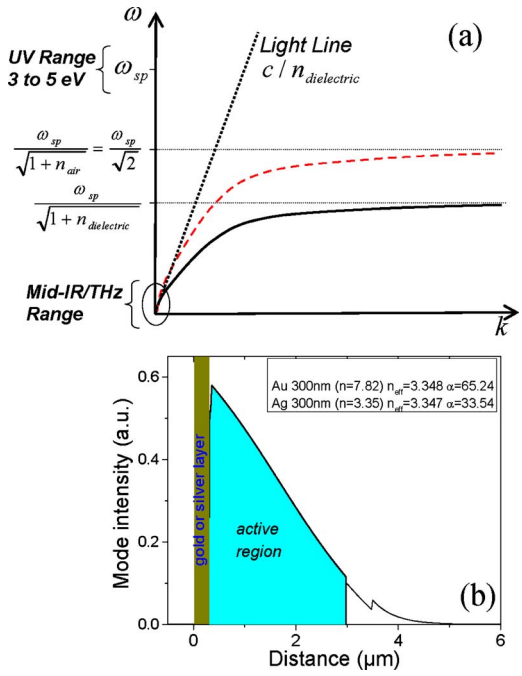

FIG. 1. (a) Schematic dispersion of surface-plasmon waves at a metal-air interface (dashed line) and at a semiconductor-metal interface (solid line). ω_{sp} is the metal bulk plasmon frequency, which typically lies in the 3–5 eV range. The nonradiative nature of surface plasmons stems from the position of the dispersion relation, which lies below the light line (thin solid line). The range of interest for our devices (mid-IR) is located close to the origin, where the surface-plasmon dispersion is acousticlike and it is tangential to the corresponding light line. (b) Intensity profile of the surface-plasmon waveguide. The waveguide losses—calculated for different metal carrier layers—are reported in cm^{-1} in the top-right inset.

doped ($n=1\times10^{17}$ cm^{-3}) InP buffer layer was used. Further details of the growth process can be found in Ref. 8. The active regions used are based on a standard two-phonon-resonance design, where the lasing transition has been designed to emit at 7.5 μm. A total number of 50 active-region/injector stages were grown, preceded by a 500-nm-thick InGaAs layer doped to $n=5\times10^{16}$ cm^{-3} and followed by contact facilitating layers.

A silver-based contact layer was used for the surface-plasmon waveguide because of the desirable refractive index properties of this metal. From Eq. (1), it can be seen that in order to achieve an efficient device operation (low waveguide losses) for a particular wavelength, it is essential to minimize the value of n_m/k_m^3. Previous surface-plasmon QC lasers operating at $\lambda\sim11$ μm utilized either gold- or palladium-based metallization for the waveguide. Table I summarizes the n_m and k_m values for gold (Au), palladium (Pd), and silver (Ag). The low value of n_m/k_m^3 for silver relative to the other metals suggests that a significant improvement in device performance can be obtained by using a silver-based surface-plasmon waveguide.

In order to quantify the expected improvement further, we simulated the optical mode profile, as shown in Fig. 1(b). The dielectric constants for the doped semiconductor layers were calculated using a Drude-Lorentz model, while the values for the metals were taken from Ref. 9. The calculations were performed for the two different metal contacts used in the present work: gold and silver. As shown in the inset of Fig. 1(b), the calculated waveguide losses are lower for a silver-based waveguide. We believe that the control mechanism for this effect is not dominated by the imaginary part of the metal refractive index, but rather by the real part. The large difference in n_m (see Table I) can induce large changes of the waveguide losses, and therefore of the device threshold current density.

TABLE I. Real and imaginary parts of the refractive index for metals used in the present work and in Ref. 7 for a QCL operating wavelength of $\lambda\sim8$ μm. All values are from Ref. 9. Equation (1) shows that the propagation loss is proportional to n_m/k_m^3. Surface plasmon waveguides utilizing silver have lower losses than gold- or palladium-based waveguides.

Metal	n_m	k_m	n_m/k_m^3
Gold (Au)	7.78	57	4.2×10^{-5}
Palladium (Pd)	3.13	36	6.7×10^{-5}
Silver (Ag)	3.35	57	1.8×10^{-5}

The wafer was processed into a range of laser ridge widths (13, 17, 21, and 25 μm), following the procedure in Ref. 10. The sample was cleaved into two parts before the top-contact metal evaporation. On one half a simple Ti/Au contact (3/300 nm) was deposited, while on the other half a Ti/Ag/Ni/Au contact (3/150/10/250 nm) was used instead. The thickness of the Ti layer is nominally the same in the two cases (3 nm). The skin depth of 7.5 μm radiation into silver was calculated to be $\approx$10 nm, therefore the nickel and gold layers have no influence on the surface-plasmon waveguide mode.

The light-current (*L-I*) characteristics [Figs. 2(a) and 2(b)] allow the evaluation of the effect of the two different surface-plasmon carrier layers (Au or Ag) on the laser performance. The Au-based lasers operate up to a maximum temperature of 260 K [Fig. 2(a)], with peak powers of $\approx$70 mW at 78 K for the case of a 21 μm wide device. On the other hand, the Ag-based lasers operate up to room temperature (300 K), with peak powers of $\approx$30 mW (78 K) for a narrower 12 μm wide device. Typical laser emission spectra for the Ag-based sample are reported in Fig. 3. The laser emission wavelength at 78 K is $\approx$7.5 μm, in excellent agreement with the band-structure calculations. In order to verify our results a large number of devices were fabricated and tested. The threshold current density for the Au-based devices tested lies in the range 2.9 ± 0.4 kA/cm^2, while for the Ag-based devices we measured 1.5 ± 0.2 kA/cm^2.

The improvement in laser performance brought about by the silver contact layer is corroborated by the characteristic temperature T_0 that can be obtained with an exponential fit of the curve $J_{th}=Ae^{T/T_0}$. We obtain 65 K for the Au-based lasers, and 120 K for the Ag-based ones.

At 78 K, the average threshold current density is approximately twice as large for the Au-based devices ($J_{th}=2.9$ kA/cm^2) than for the Ag-based ones ($J_{th}=1.5$ kA/cm^2), as shown in Fig. 2(c). The reduction of J_{th} for the Ag-based QCL is in agreement with the waveguide mode calculations (taking into account the mirror losses), when the values from Table I are used for the *real* part of the index of refraction of the two metals. However, while the ratio between the waveguide losses can be accounted for by the theory, their absolute values do not agree with the predicted values. We calculate a value $\alpha=6$ cm^{-1} for the losses, and $\Gamma=60\%$ for the confinement factor in a 7.5 μm QC laser in a standard waveguide configuration. For the same active region embedded in a Ag-based surface-plasmon waveguide we obtain instead $\alpha=33$ cm^{-1} and $\Gamma=82\%$. The figure of

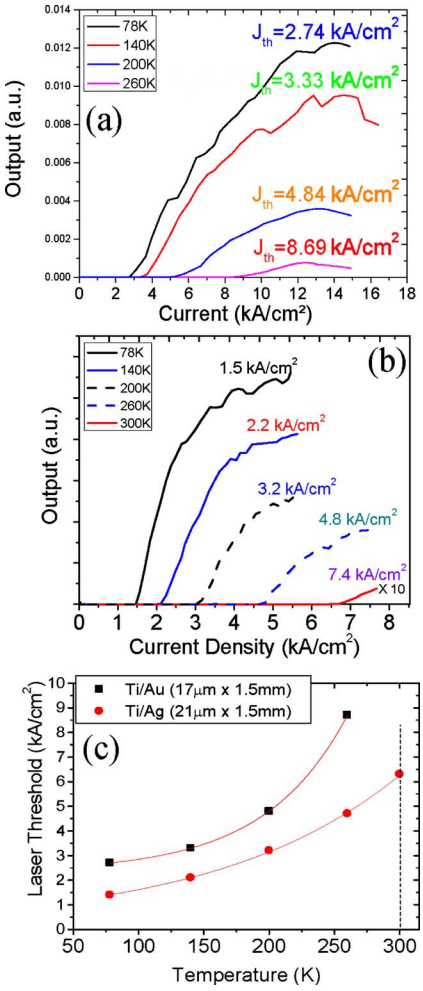

FIG. 2. (a) *L-I* characteristics of a typical laser with (Ti)/Au top contact at different heat sink temperatures. The ridge dimensions are 17 μm $\times$1.5 mm. The laser was operated in pulse mode (75 ns at 5 kHz repetition rate), and the signal was detected with a HgCdTe detector. (b) *L-I* characteristics of a typical laser with a (Ti)/Ag/Ni/Au top contact at different heat sink temperatures. (c) Threshold current densities as a function of operating temperatures for typical (Ti)/Au and (Ti)/Ag/Ni/Au devices. An improvement of approximately a factor of 2 has been obtained using Ag-based electrical contacts.

merit (defined as Γ/α) is therefore 0.1 for the former, and 0.025 for the latter. Using 1.5 kA/cm^2 as a baseline threshold at 78 K for the surface-plasmon devices, this would imply a $J_{th} \approx 500$ A/cm^2 at 78 K for a standard 7.5 μm QC laser. Such a low value was never measured for MOVPE-grown QC lasers. We believe therefore that an additional mechanism that is not currently included in the calculations, and that we have yet to identify, must be responsible for the low absolute value of J_{th} exhibited by the silver-based metallic waveguides. As the waveguide losses depend strongly on the nature of the semiconductor-metal contact interface it is likely that the effect originates from the properties of the metal layer within a few nanometers of the top semiconductor surface. We observed that the Ag-based contacts have poor adhesion properties. A nonuniform adhesion of the top

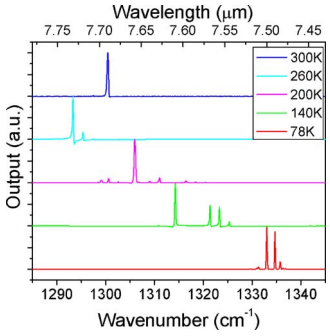

FIG. 3. Pulsed (50 ns pulse width, 84 kHz repetition rate) emission spectra for a typical device with an Ag-based surface-plasmon waveguide. The spectra were measured in rapid scan using a Nicolet fourier transform infrared spectrometer. The spectral resolution was set to 0.125 cm^{-1}.

silver would result in a lower average refractive index of the contact layer, effectively lowering the waveguide losses. We are presently undertaking further, more detailed characterization including direct loss/gain measurements.

In conclusion, we have demonstrated pulsed, room-temperature operation of surface-plasmon quantum cascade lasers at an emission wavelength of 7.5 μm. The result has been obtained thanks to a dramatic reduction of the waveguide losses, following the use of silver as both the top electrical contact and a surface-plasmon carrying layer. Such laser material is ideal for photonic-crystal applications, given its reduced thickness, maximum of the electric field at the top surface (for efficient vertical emission), and pulsed, room-temperature operation (for easy access to the laser photonic-crystal cavity for sensing/microfluidics applications).

The authors thank F. Julien, C. Sirtori, O. Painter, Y. Chassagneux, and A. de Rossi for useful discussions. R.C., V.M., and M.B. acknowledge support from the EURYI "Young Investigator Award" program. This work is supported by the UK Engineering and Physical Sciences Research Council and by the Royal Society. The device fabrication has been performed at the "Centrale Technologique Minerve" at the *Institut d'Electronique Fondamentale*.

[1] H. Raether, *Surface Plasmons on Smooth and Rough Surface and on Gratings* (Springer, Berlin, 1988).
[2] J. B. Pendry, L. Martín-Moreno, and F. J. Garcia-Vidal, Science **305**, 847 (2004).
[3] W. L. Barnes, A. Dereux, and T. W. Ebbesen, Nature (London) **424**, 824 (2003), and references therein.
[4] P. Andrew and W. L. Barnes, Science **306**, 1002 (2004).
[5] K. Okamoto, I. Niki, A. Shvartser, Y. Narukawa, T. Mukai, and A. Scherer, Nat. Mater. **3**, 601 (2004).
[6] J. Seidel, S. Grafström, and L. Eng, Phys. Rev. Lett. **94**, 177401 (2005).
[7] C. Sirtori, C. Grachl, F. Capasso, J. Faist, D. L. Sivco, A. L. Hutchinson, and A. Y. Cho, Opt. Lett. **23**, 1366 (1998).
[8] A. B. Krysa, J. S. Roberts, R. P. Green, L. R. Wilson, H. Page, M. Garcia, and J. W. Cockburn, J. Cryst. Growth **272**, 682 (2004).
[9] E. S. Koteles and W. R. Datars, Can. J. Phys. **54**, 1676 (1974); Solid State Commun. **19**, 221 (1976).
[10] V. Moreau, A. B. Krysa, M. Bahriz, L. R. Wilson, R. Colombelli, D. G. Revin, F. Julien, J. W. Cockburn, and J. S. Roberts, Electron. Lett. **41**, 1175 (2005).